JOURNAL OF SPACECRAFT AND ROCKETS
Vol. 32, No. 4, July–August 1995

Simulation of Chemically Reacting Flowfields Around a 70-deg Spherically Blunted Cone

Michael A. Gallis* and John K. Harvey†
Imperial College of Science, Technology, and Medicine, London SW7 2BY, England, United Kingdom

Results are presented from a numerical study of the flowfield around a 70-deg blunted cone using the direct simulation Monte Carlo method. For the simulation of energy exchange, chemical reactions, and ionization, the maximum-entropy method is used. The effects of chemical reactions, and ionization on the heat transfer and pressure coefficient of the flow are evaluated. This study focuses on the wake flow, and the effects of nonequilibrium thermochemical phenomena are examined. Two re-entry cases, typical of those conditions, are considered. The freestream conditions correspond to flight at an altitude of 85 km and velocities of 6.7 and 10 km/s. The enthalpy of the flow in these cases allows the full band of nonequilibrium phenomena to be initiated with varying significance. The lowest-enthalpy case is compared with the flowfield that would result if the reactions were inhibited, thus demonstrating the effects of chemical reactivity at the threshold where such effects are just noticed.

Introduction

ENVISAGED space missions will include reentry into the Mars and Earth atmospheres. To achieve a more efficient exploitation of the vehicle's payload capacity, future re-entry vehicles will be designed to use the atmosphere for maneuvering and aerobraking. The interaction of the wake area of the flowfield with the base of the vehicle affects the design of the payload compartment. Although the pressure is very low, the recirculation of high-temperature particles gives rise to significant heat transfer to the payload compartment.

The temperatures in this area may well be high enough to initiate chemical and ionizing reactions. Although the bulk of the ionization of the flow will take place in front of the body, sufficient electrons may also be produced in the wake to interfere with the antennas located at the back of the body and disrupt radio communications.

If the temperature of the flow in the wake is high enough for free electrons to electronically excite the air species, these will in turn radiate in the optical band of the spectrum. Radiative heating of the base area may be quite significant, since in the same area the convective heating drops because of the rarefaction. This problem becomes more important for atmospheres such as that of Jupiter, where it has been shown that the radiative heating in the wake can be 6% (Park[1]) of that at the vehicle stagnation point. The calculation of the radiative heating in this area is essential for the design of the heat shield at the back of the body. The disturbance area of the wake where these phenomena take place extends to several body diameters behind it. It is expected that it is only around 100 body diameters downstream that the flow cools down to the temperature of the ambient air.

For flight in the upper atmosphere, say above 50 km, the rarefaction of the flow behind the vehicle (typically the density can be a tenth of the freestream density) will give rise to significant nonequilibrium effects. The flow cannot be described by a single temperature, and chemical phenomena will depend on the internal energy states that the colliding particles occupy. The numerical prediction of such flowfields becomes particularly important in that measurements under these conditions are very difficult to make and very expensive. It is of paramount importance that the method used to predict the flowfield should be able to allow for the effects of nonequilibrium. The scope of this paper is to study the effects of chemical reactions on the flowfields of 70-deg spherically blunted cones and to compare the predictions of the maximum-entropy method with these of other available methods.

Nonequilibrium Energy Exchange

The distribution of the internal energy states, which under conditions of equilibrium is a trivial matter, becomes a complicated quantum-mechanical problem under conditions of nonequilibrium. For nonreacting flows it is valid to assume that after a collision the distribution of energy states is very close to the local equilibrium distribution. In the context of direct simulation Monte Carlo calculations it has been shown that this assumption gives reliable results.

Dealing with energy exchange after chemical reactions is not so simple. Most reactions have a tendency to distribute energy in an uneven manner, favoring one particular energy mode or certain states of an energy mode. It takes several subsequent nonreacting collisions for such a highly non-Maxwellian or non-Boltzmann distribution to reach the levels of an equilibrium one. In rarefied flows where collisions are infrequent, this results in particles "flying" for long distances with their energy content corresponding to nonequilibrium distributions. The use of the equilibrium distributions for the energy distribution after a chemical reaction is therefore inappropriate under such conditions. The derivation of the energy content of a particle after a reactive collision can be done if the potential function controlling the interaction is known. However, in most cases of interest these functions are unknown, so we have to define the most probable energy distribution in an alternative way.

Experimental results of Levine and Bernstein[2] have shown that the internal energy distribution after a reaction can be described by a simple function comprising a Boltzmann-like distribution multiplied by an exponential factor. This distribution can be derived mathematically by means of quantum mechanics based on the entropy that is associated with each distribution. The method of Ref. 2, hereafter called the maximum-entropy (ME) method, was modeled[3] in such a way that it can be applied to the DSMC algorithm.

The ME method does not assume equilibrium distributions for the translational and internal energies of the particles after the interaction, but it calculates the most probable ones in the form of a skewed Boltzmann distribution.[4] The energy distribution formulas are given as a function of a parameter, which is specified for each interaction. It has been proved[5] that under conditions of equilibrium, as expected, the ME method predicts the Boltzmann distribution as the most probable one.

Nonequilibrium Chemical Reactions

Under conditions of equilibrium, the rate at which chemical phenomena take place depends on the temperature of the flow, but under conditions of nonequilibrium the idea of a single temperature breaks down. Furthermore, it has been observed that each chemical reaction

Received March 24, 1994; revision received Aug. 11, 1994; accepted for publication Aug. 15, 1994.

*Research Associate, Department of Aeronautics. Member AIAA.
†Professor of Gas Dynamics, Department of Aeronautics. Member AIAA.

may be favored by a specific energy mode and be relatively insensitive to others. For example, dissociation reactions are enhanced by the amount of vibrational energy the reagents have. In the same way, not all reactions dispose energy in the same manner but present a preference for the specific energy modes that can initiate them.

The postcollision energy disposal and the energy preference of a chemical reaction are related to each other. This relationship can be quantified in terms of the ME approach. According to Levine and Bernstein,[2] the principle of microscopic reversibility requires that the same measure that can be applied for the calculation of the probability of a state being occupied can be applied to estimate the probability of a certain internal energy state causing a reaction.

When applied to the prediction of chemical and ionic reactions, ME gives internal-energy-state-dependent reaction probabilities and hence state-dependent reaction rates. Our current modeling using the ME approach considers the cases of the reaction rate depending only on the vibrational energy and translational energy. This limitation was imposed only to avoid unnecessary computational overhead, since predominantly these two modes control the air reactions. This limitation could be overridden by considering the probability of the rotational modes contributing to the reaction probability. In this study, the three-body recombination reactions, including recombination on the body surface, have been omitted from the reaction set, since they are very rare in low-density flows. Their significance even in the high-density areas is not considered to be very large.

Ionization of the Flows

In the study of chemically reacting flowfields, the production of ions and electrons in the flow becomes particularly important, as it changes the behavior of the flow significantly. The ionization reactions have a large effect on the temperature of the flow, since their threshold is greater than for any other chemical reaction. Recombination of the ions that hit the surface is assumed in this study, and it can be expected to increase the heat-transfer coefficients, since the neutralization energy is transferred to the surface. This mechanism constitutes an additional thermal load on the surface.

In the context of a DSMC simulation, the electrons require special treatment. Free electrons move with speeds that are typically 3–4 orders of magnitude greater than the average speed of the particles. Such high speeds require a greatly reduced computational time step to deal specifically with electrons (which account for 2–3% of the total number of particles in the flow), and this would impose a large overhead in the computation. Therefore, in this study, the electrons are assumed to move together with ions in pairs, although they keep their own true velocity for all other purposes.

The velocities of charged particles have to be modified to include the effect of Coulomb interaction with neighboring particles. In this study, where the charged particles diffuse under conditions of ambipolar diffusion, the electron-flux method (Gallis and Harvey[6]) is used. According to this method, the velocity of the electrons is calculated in such a way that the electrons keep their thermal velocity while their average velocity is modified to be equal to the ion velocity. This method has been shown[6] to satisfy all conditions of ambipolar diffusion.

Nonequilibrium Thermal Radiation

The presence of highly energetic electrons in the flow is followed by the emission of thermal radiation from the flow. Electrons are very efficient in exciting the electronic modes of heavy particles. The species that can be excited in air are N_2, O_2, N_2^+, NO, N, and O.

The calculation of the electronic excitation probability is made with the use of corresponding cross sections.[7] A collection of these has been established using the most reliable measurements or theoretical data. With the aid of these cross sections, the probability of electronic excitation is calculated for every possible state. Every time that a sufficiently energetic collision exceeds the threshold of some transitions, one of the possible states is selected using weighted probabilities. In the case of a successful excitation event, the particle is excited to the energy level in question. Thus the use of any assumed distribution of the energy states is avoided.

From a previous study (Gallis and Harvey[7]) the radiation emission was found to be important only in a very limited area of the shock wave around the stagnation streamline, where the maximum electron density and temperature overlap. In that area it was found that the radiation emission peaked sharply. Although the radiation emission was predicted to be of order of 1 MW/m^3, the area where it appears is rather small, reducing therefore its effect on the temperature and the radiative heat transfer.

Viking Test Case

There are a large number of aerobrake vehicles that have been proposed for the future entry missions. Although these configurations have several differences in their design, they all agree in comprising a spherically blunted cone and a backbody payload. The angle of the cone varies with the type of vehicle. Most of the configurations, though, seem to agree on a 60 or 70 deg cone. Lately the 70-deg cone has received a great deal of attention[8,9] due to its selection by an AGARD working group as the most appropriate shape for special investigation.

This configuration (see Fig. 1) was selected for the present study. A 2-m-diam body was used. In order to evaluate the effects of chemical reactions on the flowfield of the vehicle, three cases were studied. All three correspond to flight at 85 km with velocities from 6.7 to 10.0 km/s. The ambient air conditions for these test cases are presented in Table 1.

In the third case studied, chemical reactions were inhibited. The conditions of this case are the same as those of case 2, i.e., for 6.7 km/s. The aim of this third case is to identify the effects of chemical reactions in a flowfield close to the threshold where these first take place. The conditions of the simulations are presented in Table 2.

Computations for an axisymmetric flow have been performed with approximately 500,000 particle simulators on a grid of 12,330 cells, which covers an area 6 m long and 5 m wide. The grid used is shown in Fig. 2. Layers of fine cells were used on the surface of the body to capture the density gradients that are met in that region. Other calculations made by the authors, which are not presented in here, with a smaller number of cells (10,000), gave roughly the same reults. It is believed therefore that the presented results do not depend on the grid resolution. All of the contour and profile data presented are completely unsmoothed unless otherwise stated. The values in the profile plots have been normalized with the freestream values.

Table 1 Ambient air conditions

Altitude	85 km
Freestream temperature	180.65 K
Number density	1.7090×1030 m^{-3}
Mean free path	9.9958×10^{-3} m
Wall temperature	1000 K

Table 2 Conditions of simulations

Case	Speed, km/s	Reactions
1	10.0	Yes
2	6.7	Yes
3	6.7	No

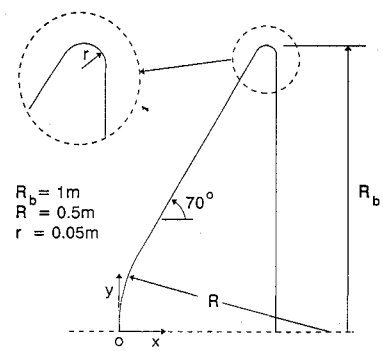

Fig. 1 Viking configuration.

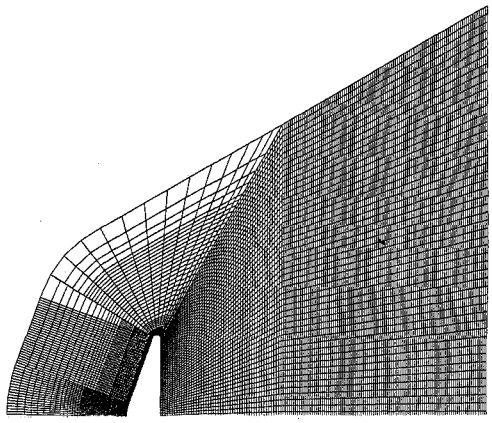

Fig. 2 Computational domain and grid.

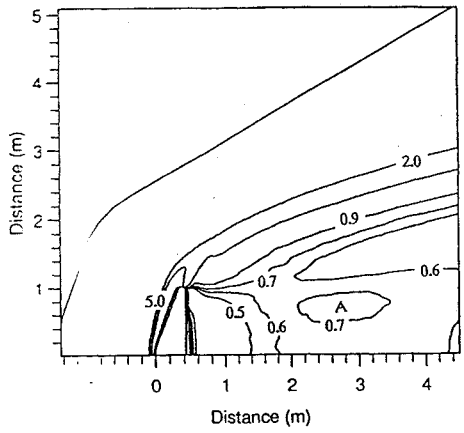

Fig. 3 Density contour lines for case 1.

Discussion of the Results

Case 1: 10 km/s

The first case is for the highest enthalpy of all three simulated. Flows at around 10 km/s have enough energy to initiate the 41 most significant chemical and ionic reaction of interest in (N_2, O_2) air flows. As a result of these reactions, the simulated air is a mixture of 11 species, including the electrons. The fact that the energy of the flow is enough to initiate all of the physical processes included in the code makes this case particularly interesting.

Figure 3 shows the density contour lines for this case. In front of the body, a shock wave is formed, which extends behind it, surrounding the wake area. Figure 3 shows a high-density area immediately behind the body, which is created by the recirculation of the particles in the wake. The density in this area reaches a value about 90% of the freestream density. At about $x = 3$ m, there is a very diffuse recompression shock, which increases the density even further. This results in the formation of a torroidal region (A) at a radius 0.9 m, surrounding the axis of symmetry, where the density peaks to around 70% of the freestream density. In the radial direction, the density rises again because of the presence of the conical shock layer which surrounds the wake area.

Figure 4 shows profiles of density and temperature along the stagnation line. The flow is from the left to the right. Because of the rarefaction of the flow at 85 km, no distinct shock wave is formed in front of the body. Instead, a diffuse compression layer is produced in which the density rises smoothly, accelerating sharply near the surface. Far greater densities are found in front of the body than in the wake, and the density reaches a value of about 120 times the freestream density.

The backscattered particles that diffuse upstream cause the temperature to rise. The translational temperature starts rising at $x = -0.25$ m in what might be termed a thermal shock wave, and reaches a peak of 200 times the freestream temperature. The rotational temperature lags behind the translational and starts rising at $x = -0.20$ m. The rotational temperature reaches a maximum of

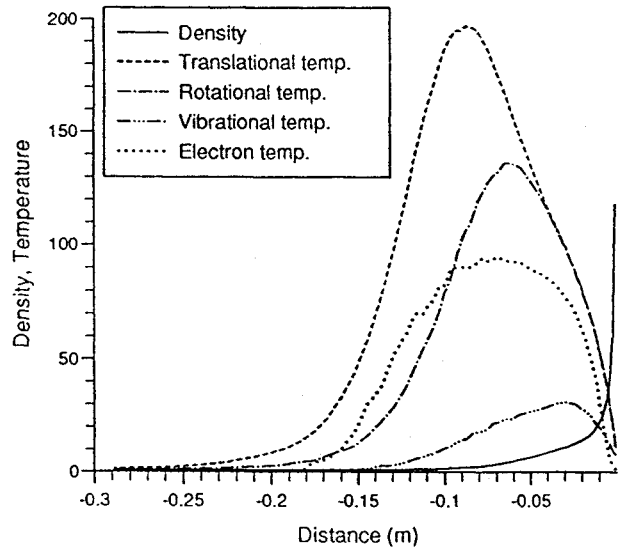

Fig. 4 Density and temperature profiles along the stagnation streamline for case 1.

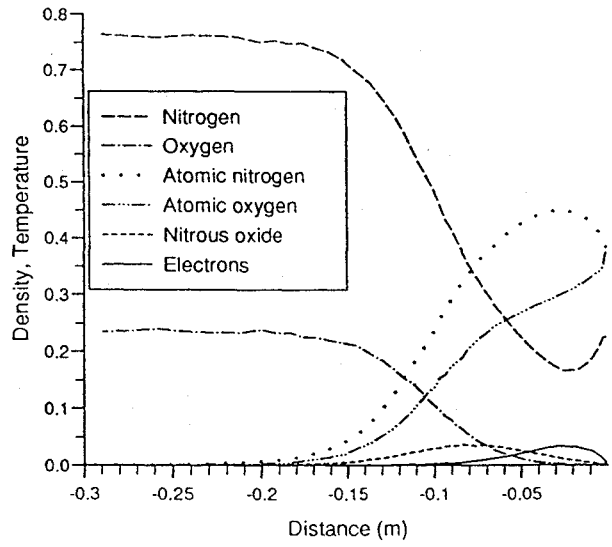

Fig. 5 Main species mole fraction along the stagnation streamline for case 1.

140 times the freestream temperature. The vibrational temperature, which under normal conditions would be almost frozen at this altitude, is initiated by the chemical reactions and starts rising at $x = -0.15$ m. It reaches a peak of 35 times the freestream temperature behind the peak of the rotational temperature. In Fig. 4, the electron temperature is presented as well. The electron temperature, which is the translational temperature of the free electrons in the flow, follows the rotational temperature closely and peaks at about 100. The statistical noise in this profile is more significant than in the others, because of the small percentage of electrons in the flow, and slight smoothing has been applied by averaging over three adjacent cells.

We notice from this plot that nowhere within the flowfield is thermodynamic equilibrium achieved. It is only at the surface of the vehicle that the three temperatures are equilibrated. The electron temperature is zero, as complete neutralization of charged species at the surface is assumed.

The high temperatures that are met in the flowfield initiate chemical and ionizing reactions. The variation of the chemical synthesis of the flow along the stagnation streamline is shown in Fig. 5. The flow is from the left to the right. At around $x = -0.15$ m, simultaneously with the beginning of the rise of the vibrational temperature, the molecular species start to dissociate. The mole fraction of the atomic species increases until it reaches the ionization area, where the increase rate is greatly reduced. The appearance of the atomic species in the flow is followed by the formation of NO in the area of the

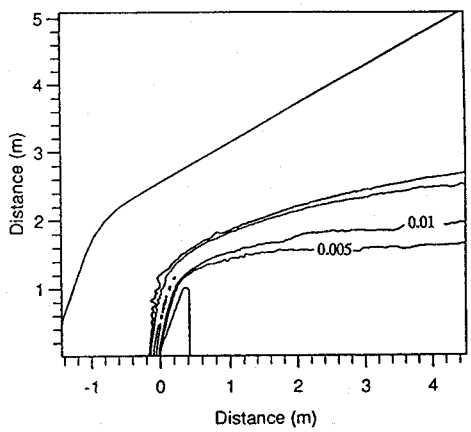

Fig. 6 NO mole fraction contour lines for case 1.

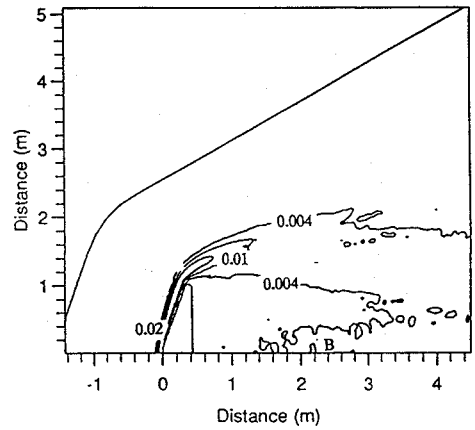

Fig. 7 Electron mole fraction contour lines for case 1.

shock layer. When the mole fraction of NO has reached its peak value of around 4%, the first electrons appear in the flow. Ionization takes place between the area where the chemical reactions take place and the surface of the body. The electron mole fraction, which equals that of the ionic species as well, reaches a maximum of 3.5%.

The mole fractions in the flowfield of NO and electrons, the last products in the chain of chemical and ionic reactions, are presented in Figs. 6 and 7, respectively. From Fig. 6, we note that NO is only formed in front of the body. Chemical reactions seem to freeze around the corner of the body, after which the mole fraction of NO remains almost unchanged in the shock layer. The behavior of the electrons is similar, but they, being more mobile, diffuse into the rarefied area of the wake behind the body. Figure 7 shows the formation of a cylindrical ionized area (B) around the line of symmetry behind the body. The mole fraction of the electrons in this area is very small (0.4%). Nevertheless, since in real cases the payload and the radio antennas are located at the back of the body, this small mole fraction of electrons is enough to cause noise in radio communications.

In Fig. 8 the contour lines for the vibrational energy are presented. As expected, the highest vibrational energy is reached in front of the body, where the flow is chemically very active. The expansion around the tip of the body into the wake freezes both vibrational temperature and chemical reactions. Virtually no activity takes place behind the body.

Case 2: 6.7 km/s

The second case is for a lower enthalpy than the first one simulated. The energies involved are at the threshold where reacting-gas phenomena start to become important.

The velocity of this case is approximately 70% of the first case and results in the formation of a weaker shock. The densities, therefore, both in front of and behind the body, are significantly reduced. Within the wake, the density reaches a maximum value of 60% of the freestream density (Fig. 9a). It is worth noting that similar simulations by Dogra et al.,[9] presented in Fig. 9b with DSMC and

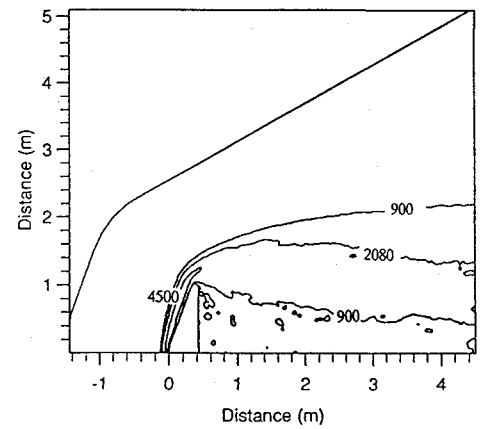

Fig. 8 Vibrational temperature contour lines for case 1.

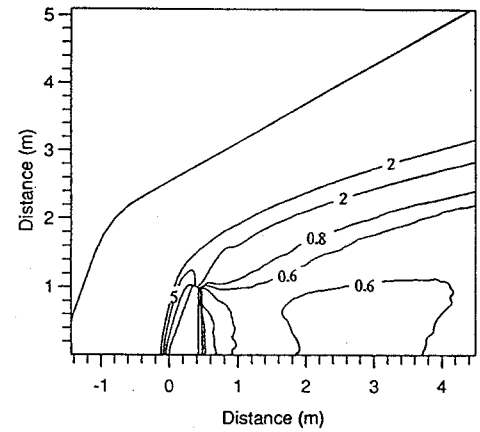

a)

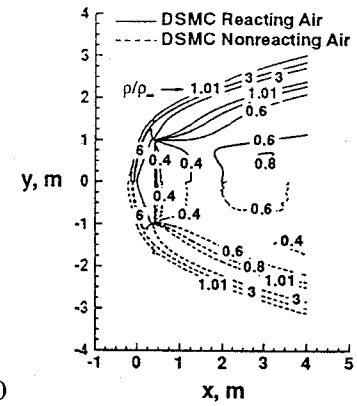

b)

Fig. 9 a) Density contour lines for case 2 and b) density contour lines from the Dogra calculations.

Navier–Stokes solvers, presented the formation of such a region in the wake (Fig. 9b has been taken from Ref. 9), though the flowfields looked very similar in general. The Dogra simulation was performed for velocity of 7 km/s and the same altitude as the current one. Further details about the simulation can be found in the references. The density on the stagnation line (Fig. 10) peaks at around 80 times that of the freestream. Comparison of Figs. 4 and 10 shows that the positions where the distributions of temperatures along the line of symmetry start rising are not greatly influenced. It is only the maximum values of these properties that change significantly.

The molecular species (Fig. 11) dissociate along the stagnation streamline to a smaller degree, with oxygen in this case not reaching complete dissociation. The mole fraction of oxygen reaches a minimum of 5%. The production of NO is not greatly influenced, and it reaches the same mole-fraction levels as in the previous case. The ionization is only very slight, and its maximum on the stagnation streamline is only about 0.5%. The flow pattern of NO in the previous case was repeated here, as can be seen in Fig. 12. This is not the

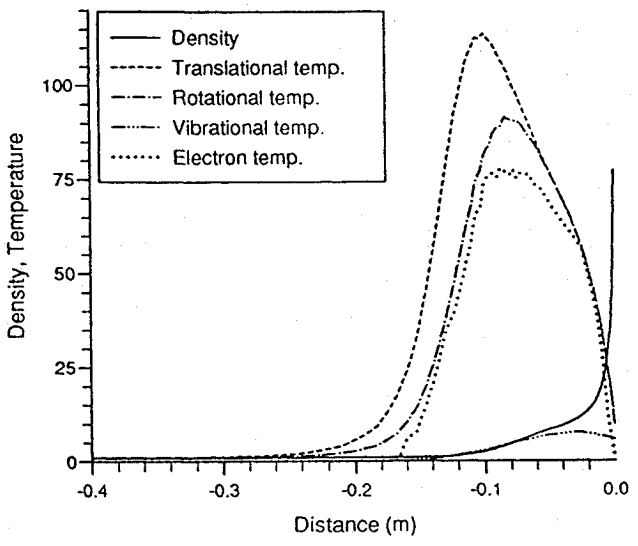

Fig. 10 Density and temperature profiles along the stagnation streamline for case 2.

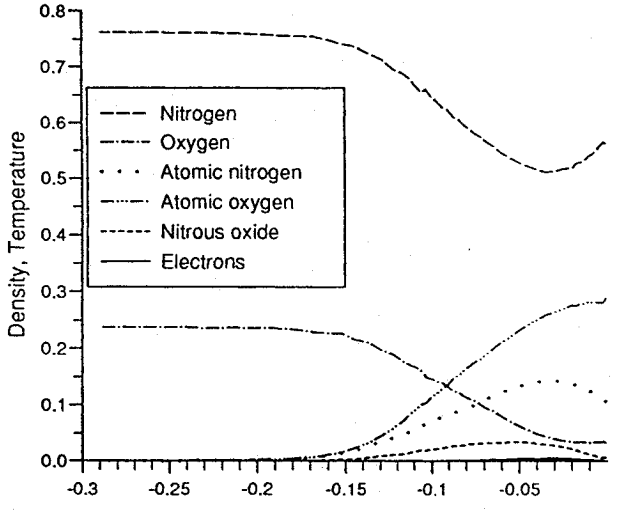

Fig. 11 Main species mole fractions along the stagnation streamline for case 2.

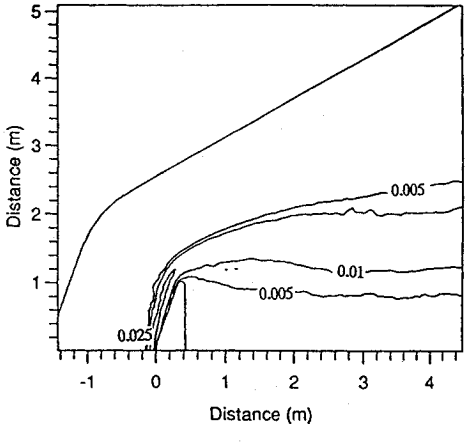

Fig. 12 NO mole fraction contour lines for case 2.

case with the distribution of the ionic species. The maximum mole fraction of electrons in the wake (Fig. 13) was very low (0.05%). Diffusion of the wake electrons towards the line of symmetry would lead to even smaller mole fractions near the axis, which are beyond the resolution of the simulation. The distribution of vibrational energy in the flowfield (Fig. 14) follows the pattern of the previous case with the corresponding values reduced.

Figures 15a and 15b (Fig. 15b has been taken from Ref. 9) present the molecular nitrogen mole fractions as found in this calculation

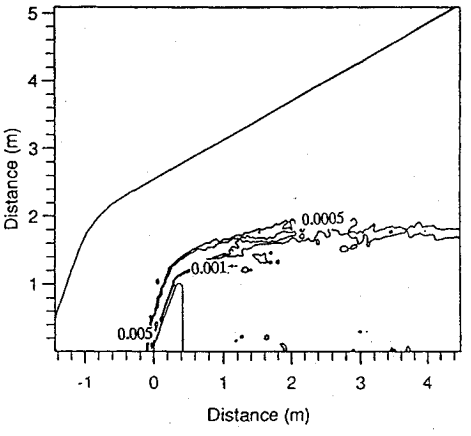

Fig. 13 Electron mole fraction contour lines for case 2.

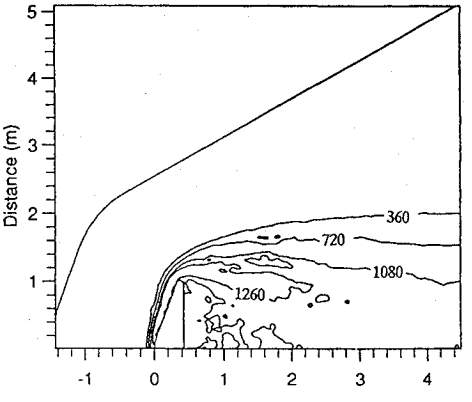

Fig. 14 Vibrational temperature contour lines for case 2.

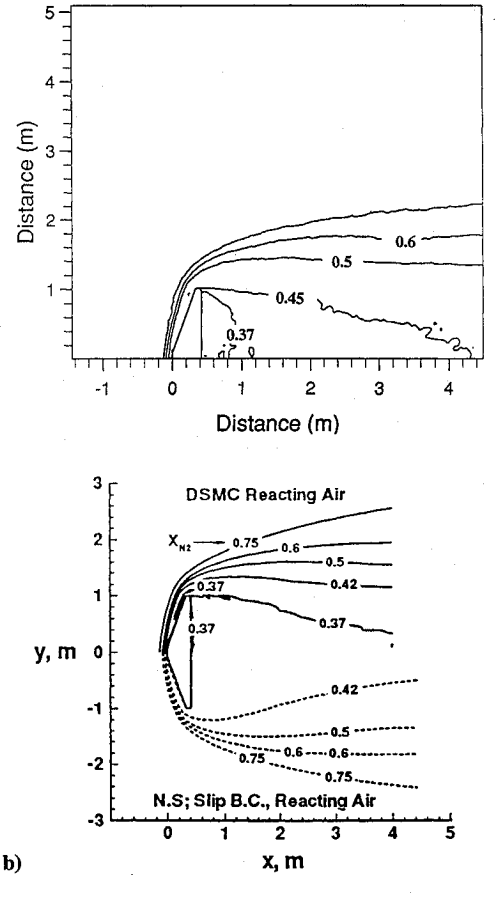

Fig. 15 a) Molecular nitrogen mole fraction for case 2 and b) molecular nitrogen mole fraction, Dogra calculations.

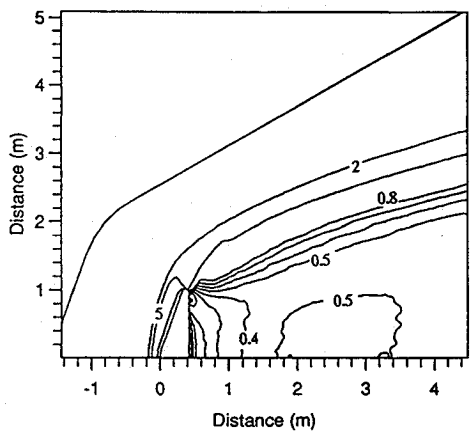

Fig. 16 Density contour lines for case 3.

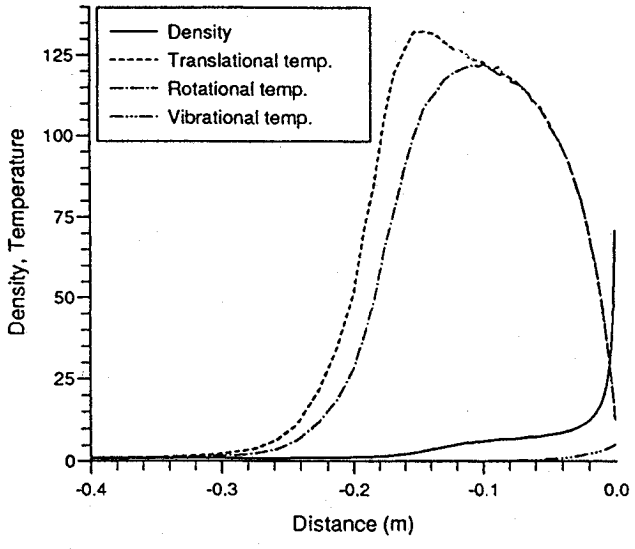

Fig. 17 Density and temperature profiles along the stagnation streamline for case 3.

and in the Dogra calculation. From the comparison of these two figures we can see that the current calculation presents a lower degree of dissociation of molecular nitrogen in the wake area. This should be expected, since the current simulation uses a vibrational-energy-favored model for the chemical reactions, whereas in the Dogra calculation the equilibrium chemistry model by Bird was used, which does not discriminate between the energy modes. Since the vibrational energy of the flow in the wake drops to relatively low values, the chemical activity is reduced. The low vibrational energies make the process of the nitrogen dissociation slow down. This explains the higher mole fraction of nitrogen in the current calculations. It is interesting to note that the current DSMC simulation seems to be in better agreement with the continuum solution of Dogra et al. than with the Dogra DSMC solution.

The low degree of dissociation in case 2 poses the question whether the computational overhead of the real-gas effects could be avoided. To answer this question case 2 was simulated with the chemical reaction inhibited. This simulation is of course unrealistic, and it was only done to compare the two cases.

The density profiles of the flowfield are presented in Fig. 16. Although the flowfield looks similar to the previous cases, the density levels within the wake area are significantly reduced. This observation is in agreement with the results of Dogra et al.[9] (see Fig. 9a). A closer look at temperature profiles along the stagnation streamline in Fig. 17 shows striking differences. The peak translational temperature standoff distance is increased remarkably without reactions from about $x = 0.10$ to 0.15 m. Since the degree of dissociation is not very large in the reacting case, the difference in the peak temperatures is only 8% higher for case 3. A more significant difference is observed in the vibrational temperature. Vibrational-energy exchange is amplified by chemical reactions, which double the peak vibrational temperature and move the peak upstream. Without chemical reactions the vibrational energy peaks at the surface of the body, because it is only there that the density is high enough to give sufficient collisions for significant energy exchange into the mode to occur. With the addition of chemical reactions, vibrational-energy exchange takes place where high temperatures exist, which moves the peak upstream. This absorption of energy by the vibrational mode and by chemical bonds results in the compression of the high-temperature area, which in turn affects the density profile. From Fig. 17 we can see that the density starts rising earlier than in case 2 ($x = -0.2$ m instead of $x = -0.14$ m) with the formation of a diffuse but distinct shock wave that is very similar to a Rankine–Hugoniot shock. The density then plateaus and starts to rise towards the surface. The peak density (75 times the freestream density) is lower than in case 2.

Thermal Radiation

The calculation of thermal radiation emitted from the flowfield was also included in the simulation. The total radiation emission was found to be significant only in a narrow region on and around the stagnation streamline. The peak readiation emission on the stagnation streamline was 0.4 MW/m^3 for the first case and 0.02 MW/m^3 for the second case. The radiation emission from the rest of the flowfield in front of the body was found to be less significant. The radiation due to electronic excitation from the wake area was found to be insignificant. The very low mole fractions of electrons did not allow sufficient electronic excitation of the heavy particles. Another source of electronic excitation, due to collisions of atoms, which could have also contributed to the emitted radiation, has not been included in the radiation model used.

Heat Transfer and Pressure Coefficients

The heat transfer and pressure coefficients on the body were calculated for the three cases. The heat transfer coefficient for all three cases are presented in Fig. 18 as a function of the length s along the surface of the body measured from the front stagnation point. From this figure, we note that the heat-transfer coefficient is reduced as we move away from the stagnation point. Around the corner of the body the heat transfer drops by 2 or 3 orders of magnitude. In the wake area near the centerline, the heat transfer coefficient is increased by one order of magnitude above the value near the top corner of the body, because of the recirculation of the flow. This increase emphasizes the importance of using the correct body geometry when studying the wake region, since the payload may influence the flow and it is likely to be a sensitive area of the vehicle.

As the flow enthalpy is increased, the flow becomes more chemically active and proportionally more heat transfer energy is convected away from the body. For case 1 the additional heat transfer mechanism of ion recombination on the surface was included. This

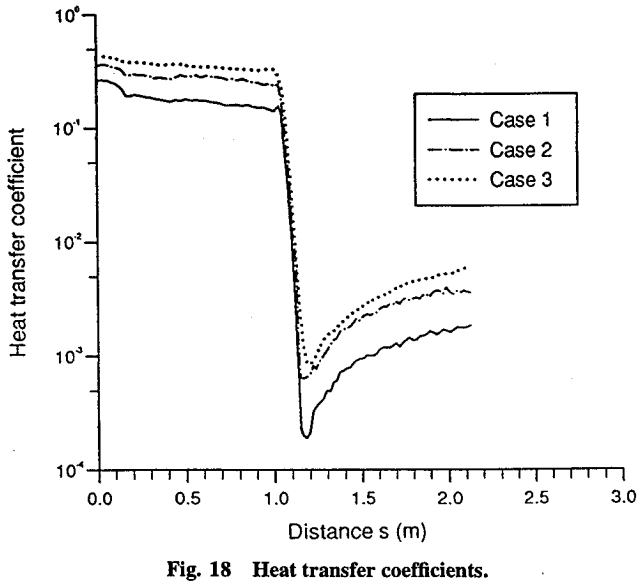

Fig. 18 Heat transfer coefficients.

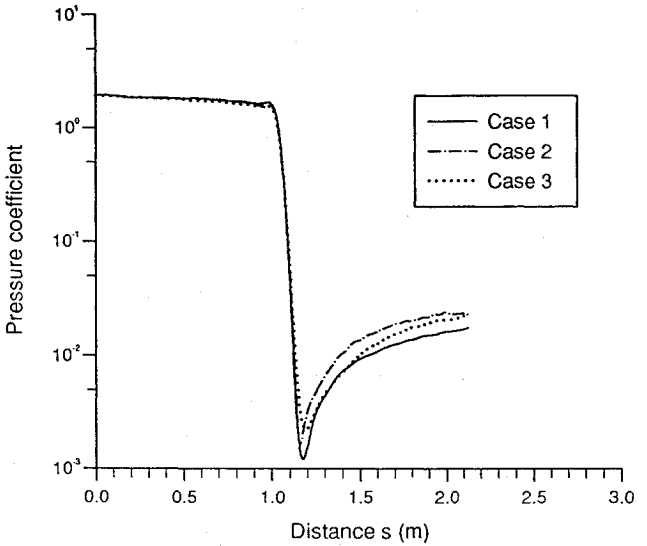

Fig. 19 Pressure coefficients.

mechanism becomes particularly important in the area of the stagnation point, where the electron layer is very close to the surface. The upward kink in the heat transfer coefficient in the vicinity of the stagnation point must be attributed to this mechanism.

The pressure coefficients are presented in Fig. 19. We note that all three cases give the same pressure distribution along the surface of the body. As expected,[10] the inclusion of the chemical reactions in case 2 did not change the pressure distribution from that in case 3. The pressure coefficient rises in the wake area in a similar manner to the heat transfer. Statistical noise was more prominent in the wake area, where the particle concentration was low.

Conclusions

Simulations have been performed for the flowfield around a 70-deg spherically blunted cone at 6.7 and 10 km/s at an altitude of 85 km in air. The computations extended to 2 diam behind the body and reveal details of the wake flow. The simulations included the effects of chemical and ionic reactions and thermal radiation. For all three cases it was concluded that thermodynamic nonequilibrium dominates the flowfield. The inclusion of the chemical and ionizing reaction was found to influence the properties of the flowfield to a very large extent. As a consequence, the heat transfer coefficient was found to be affected both in front of the body and in the area of the wake. In contrast, the pressure coefficient was little influenced by the chemical activity. Although the flow in the area of the wake was found to be slightly ionized, this did not lead to any electronic excitation and thermal radiation.

Acknowledgment

This work has been carried out with the support of the British Ministry of Defence (D.R.A. Farnborough) under Agreement AT/2037/331.

References

[1]Park, C., *Nonequilibrium Aerothermodynamics*, Wiley, New York, 1990.

[2]Levine, R. D., and Bernstein, R. B., *Molecular Reaction Dynamics and Chemical Reactivity*, Oxford Univ. Press, Oxford, England, UK, 1987.

[3]Marriott, P. M., and Harvey, J. K., "New Approach for Modelling Energy Exchange and Chemical Reactions in the Direct Simulation Monte Carlo Method," *Rarefied Gas Dynamics*, edited by A. E. Beylich, VCH, 1990, pp. 784–791.

[4]Gallis, M. A., and Harvey, J. K., "The Maximum Entropy Approach Applied to Energy Exchange, Chemical Reactions and Ionization in the Direct Simulation Monte Carlo Method for Rarefied Hypersonic Flows," Imperial College-AERO Report 93-01, ISSN 0308-7247, Imperial College, London, 1993.

[5]Marriott, P. M., Ph.D. Thesis, Univ. of London, London, Jan. 1994.

[6]Gallis, M. A., and Harvey, J. K., "Modelling of Ionization Reactions and of the Resulting Electric Fields in One-Dimensional Hypersonic Shock Waves with the Direct Simulation Monte Carlo Method," Imperial College-AERO Report 92-01, ISSN 0308-7247, Imperial College, London, 1992.

[7]Gallis, M. A., and Harvey J. K., "Nonequilibrium Thermal Radiation from Air Shock Layers Modelled with the Direct Simulation Monte Carlo Method," AIAA Paper 93-2805, July 1993.

[8]Moss, J. N., Mitcheltree, R. A., and Wilmoth, R. G., "Hypersonic Blunt Body Wake Computations using DSMC and Navier–Stokes Solvers," AIAA Paper 93-2807, July 1993.

[9]Dogra, V. K., Moss, J. N., Wilmoth, R. G., Taylor, J. C., and Hassan, H. A., "Effects of Chemistry on Blunt Body Wake Structure," AIAA Paper 94-0352, Jan. 1994.

[10]Anderson, J. D., *Hypersonic and High Temperature Gas Dynamics*, McGraw–Hill, New York, 1988.

I. D. Boyd
Associate Editor